



Azimuthal dependence of electromagnetically induced grating in a double V-type atomic system near a plasmonic nanostructure

Seyyed Hossein Asadpour^{1,a}, Teodora Kirova^{2,b}, Hamid R. Hamed^{3,c}, Vassilios Yannopoulos^{4,d}, Emmanuel Paspalakis^{5,e}

¹ School of Physics, Institute for Research in Fundamental Sciences (IPM), Lavasani Street 70, P.O. Box 19395-5531 Tehran, Iran

² Institute of Atomic Physics and Spectroscopy, University of Latvia, Jelgavas Street 3, Rīga 1004, Latvia

³ Institute of Theoretical Physics and Astronomy, Vilnius University, Saulėtekio g. 3, 10257 Vilnius, Lithuania

⁴ Department of Physics, National Technical University of Athens, Zografou Street 80, 157 Athens, Greece

⁵ Materials Science Department, University of Patras, 26504 Patras, Greece

Received: 22 December 2022 / Accepted: 6 March 2023

© The Author(s), under exclusive licence to Società Italiana di Fisica and Springer-Verlag GmbH Germany, part of Springer Nature 2023

Abstract We conduct theoretical and numerical studies of the performance of a 2D electromagnetically induced grating in a 4-level quantum system, which is situated near a plasmonic nanostructure. The plasmonic nanostructure is built by metal-coated dielectric nanospheres in a periodic 2D arrangement. The double V-type system is coupled by a weak probe laser, a spatially-dependent standing wave field and a Laguerre–Gaussian field. The plasmonic metamaterial causes quantum interference in the spontaneous emission from the two closely situated upper states, which makes the amplitude and phase modulations of the weak probe light dependent on the azimuthal angle and the orbital angular momentum of the vortex coupling beam. In the absence of the plasmonic nanostructure this behavior does not exist due to the lack of quantum interference. We demonstrate that by adjusting the parameters of the vortex beam, as well as the distance to the plasmonic nanostructure, the amplitude and phase modulations of the probe laser, and the Fraunhofer diffraction patterns of the grating can be controlled, directing the weak probe light energy to high-orders. The spatially dependent coupling light causes the Fraunhofer diffraction to have an asymmetric patterns when a negative or a positive value of the winding number is applied. Our work proposes a straightforward scheme for manipulation of the diffraction efficiency of the grating by utilizing both the winding number of the Laguerre–Gaussian beam, and the distance between the quantum system and the plasmonic nanostructure as control knobs.

1 Introduction

Plasmonic (metal) nanostructures (PNs) are defined by the so-called plasmon oscillations, i.e., collective oscillations of electrons with a certain frequency caused by external radiation. Plasmons enable strong absorption of light, scattering, as well as near-field amplification, thus rendering plasmonic nanostructures unique optical properties which have gathered extensive research interest in last years. PNs have found a wide range of applications in photovoltaics and detection [1, 2], sensing and imaging [3, 4], and field-enhanced spectroscopy [5]. Plasmon excitations have also been utilized to alter the energy and kinetics of chemical transformations [6, 7].

Strong modifications of different coherent optical phenomena have also been shown in quantum systems nearby PNs, among which optical transparency and slow light [8, 9], modified nonlinear optical switching and second harmonic generation [10, 11], as well as control of population dynamics [12, 13]. Of special interest for our work are the phase-dependent effects in multilevel quantum systems caused by the presence of PNs [14] that induce quantum interference in spontaneous emission and may potentially lead to several phenomena, including slow light [15] and controlled absorption and dispersion [16, 17].

Electromagnetically Induced Grating (EIG) [18–20] occurs when a coupling field in the form of a standing-wave (SW) is used in a typical Electromagnetically Induced Transparency scheme [21, 22]. In this case the traveling wave probe field absorption and dispersion become periodic in space, leading to transfer of the energy of the probe field to higher orders of diffraction. The specific EIG properties have given rise to novel applications in storing propagated light in atomic media [23], optical switching [24], all-

^a e-mail: asadpour@ipm.ir

^b e-mail: teo@lu.lv (corresponding author)

^c e-mail: hamid.hamed@tfai.vu.lt

^d e-mail: vyannop@mail.ntua.gr

^e e-mail: paspalak@upatras.gr

optical beam fanning [25], as well as interdisciplinary applications such as optical bistabilities [26], electromagnetically induced Talbot effect [27], multi-component vector solitons [28], and Ferris wheels for ultracold atoms [29, 30].

EIGs have also been studied in more complicated four-level configurations—tripods [31] or Y-type atomic systems [32], including our recent studies [33] in an N -scheme, where the additional interaction with optical vortices carrying Orbital Angular Momentum (OAM) [34] provides an easy tool for manipulation of the grating.

The abilities of optical vortex beams for control of atomic optical properties have been investigated in quantum information [35] and communication [36], exchange of OAM modes in quantum systems with complicated level structure [37, 38], and slowing of light using vortices [39, 40].

Combining the strong modifications of coherent optical phenomena occurring nearby PNs, the additional degrees of freedom provided by optical vortices, and the increased flexibility of multi-level atomic systems, we study 2D EIG in a four-level quantum system near plasmonic metamaterials using spatially dependent coupling light which carries OAM.

We are interested in a double V -type atomic scheme, where the PN affects one of the V -type transitions, while the other transition interacts only with the free space. We are able to derive analytically the linear and nonlinear susceptibility, due to our assumption of weak probe and coupling fields. We realize that because of the closed-loop double V -type quantum system the amplitude and phase modulations of the probe light depend on the azimuthal angle and the OAM of the vortex coupling beam. Thus, we can control the diffraction efficiency of the grating by adjusting the OAM parameter of the vortex field. In addition, we show that the diffraction efficiency can be modified by varying the distance between the quantum system and the PN. The 2D EIG based on our proposed model is advantageous compared to previous studies (for example based on spontaneously generated coherence or relative phase between the applied light), including to our recent investigations of EIGs near PNs [41, 42], by providing easily achievable manipulation of the grating performance, where the control knobs are simply the azimuthal angle and the winding number the vortex, as well as the distance between the quantum system and the PN. Such an atomic phase grating could find applications in all-optical switching at the few photons level where a quantized signal field could be used to create a grating to diffract and switch a quantized probe field. The low losses which the phase grating provides are paramount for such quantum all-optical switches, making the proposed scheme advantageous in future applications.

Eventhough the control of Fraunhofer diffraction spectrum has been studied in different systems, where the energy transfer of the probe field far above the diffraction is one of the important topics of investigation, there are some important points which distinguish our present work. The first feature is the possibility of a much higher probe field energy distribution in different areas of space by controlling the amount of vortex light for different distances between the atomic system and the plasmonic nanostructure. This feature is reported for close distances between atomic system and plasmonic nanostructure for positive and negative values of winding number. The second important novelty presented here is the use of vortex light, which provides a new degree of freedom for the asymmetric distribution of the Fraunhofer diffraction.

The paper is organized as follows. In Sect. 2 we present the theoretical formalisms, where the decay rates entering the equations of motion are modified by the presence of the PN. The further performed numerical calculations are presented in Sect. 3. There we show the Fraunhofer diffraction and the amplitude and phase modulations, using various system parameters, and make conclusions about the possible controllability of the EIG performance. Finally, in Sect. 4 we conclude our theoretical and numerical findings and discuss possibilities for future directions.

2 Theoretical formalisms

We start our investigation by presenting in Fig. 1a the double V -type quantum system consisting of two ground levels $|1\rangle$, $|2\rangle$ and two excited levels $|3\rangle$ and $|4\rangle$, similarly to previous studies [8, 14, 41, 42]. The states $|1\rangle$ and $|2\rangle$ are $J = 0$ levels while states $|3\rangle$ and $|4\rangle$ are $J = 1$, $M_J = \pm 1$ levels. The transition $|1\rangle \rightarrow |3\rangle$ is driven by a weak probe field with Rabi frequency Ω_p , while the transition $|1\rangle \rightarrow |4\rangle$ is mediated by a coherent field with standing-wave pattern with Rabi frequency Ω_c and a vortex beam with Rabi frequency Ω_v .

The distance between the plasmonic nanostructure and the 4-level quantum system is denoted by d . The surface plasmon bands of the PN affect the transitions in one of the V -type quantum systems, such that the spontaneous decay of the excited states $|3\rangle$ and $|4\rangle$ to level $|2\rangle$ becomes 2γ . At the same time, the free-space vacuum modes interact with the other V -type quantum system such that the spontaneous decay rate of the excited states $|3\rangle$ and $|4\rangle$ to level $|1\rangle$ is $2\gamma'$. As a plasmonic nanostructure we have considered a 2D array of metal-coated dielectric nanospheres, represented in Fig. 1b. In this case the relevant decay rates are calculated by a rigorous electromagnetic Green-tensor technique [43–45].

The two coherent fields with a standing wave pattern and a vortex beam are given by:

$$\begin{aligned}\Omega_c &= \Omega[\sin(\pi x/\Lambda_x) + \sin(\pi y/\Lambda_y)], \\ \Omega_v &= \Omega e^{-r^2/w^2} (r/w)^{|l|} e^{il\phi}.\end{aligned}\quad (1)$$

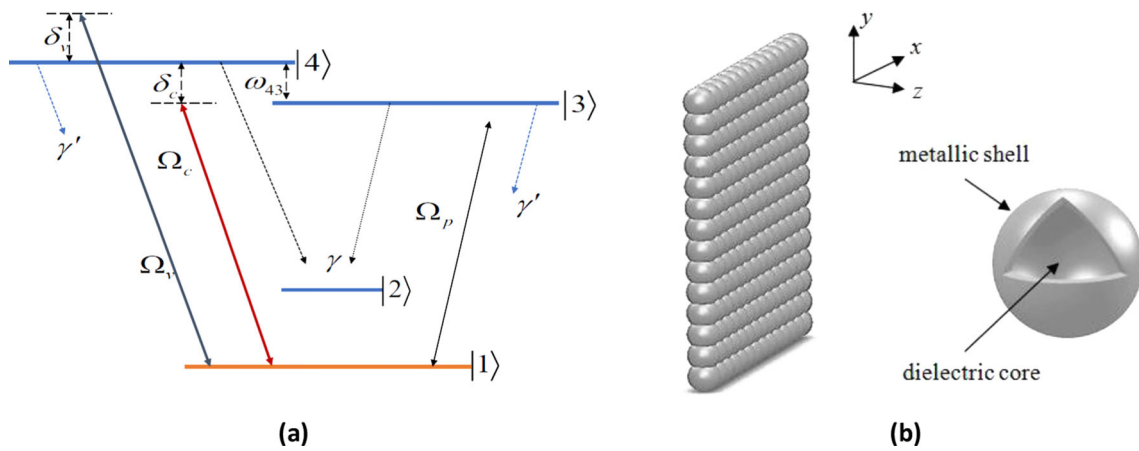


Fig. 1 **a** Double V-type atomic system interacting with a coupling light with Rabi frequency Ω_c , a vortex beam with Rabi frequency Ω_v and a probe light with Rabi frequency Ω_p ; **b** PN arranged in a 2D array at a distance d from the 4-level quantum system. More details are given in the text

In the above, Ω shows the amplitude of the fields, while Λ_x and Λ_y denote the space frequencies of the standing wave field. The parameter $r = \sqrt{x^2 + y^2}$ represents the radial distance from the axis of the vortex, $\phi = \arctan(y/x)$ is the azimuthal angle, l (integer) shows the vorticity, and w stands for the beam waist of the optical vortex.

The wave function of the system $|\Psi(t)\rangle = \sum_{i=1,4} a_i(t)e^{-i\omega_i t} |i\rangle$ can be decomposed in the basis set $\{|1\rangle, |2\rangle, |3\rangle, |4\rangle\}$ with the time-dependent coefficients $a_i(t)$ and the atomic energy $\hbar\omega_i$ of level $|i\rangle$. The equations of motion for the $a_i(t)$ coefficients are then derived upon applying the Weisskopf-Wigner theory of spontaneous emission, as well as the electric-dipole and rotating-wave approximations:

$$\begin{aligned} \dot{a}_1 &= i\Omega_p a_3 + i(\Omega_c + \Omega_v)a_4, \\ \dot{a}_2 &= i\delta_2 a_2, \\ \dot{a}_3 &= i(\delta_2 + i(\gamma + \gamma'))a_3 + i\Omega_p a_1 + \kappa a_4, \\ \dot{a}_4 &= i(\delta_1 + i(\gamma + \gamma'))a_4 + i(\Omega_c + \Omega_v)a_1 + \kappa a_3. \end{aligned} \tag{2}$$

Here, we have introduced the detunings $\delta_1 = \delta - \omega_{43}/2$ and $\delta_2 = \delta + \omega_{43}/2$. The condition $\delta_c = \delta_v = \delta$ needs to be fulfilled at all times in order for the EIG to be created [46]. The coefficient κ describes the quantum interference effects in the system via the coupling between levels $|3\rangle$ and $|4\rangle$.

According to Ref. [13], the parameters κ and γ occur due to closeness of the PN and their values are:

$$\begin{aligned} \gamma &= \frac{1}{2}(\Gamma_{\perp} + \Gamma_{\parallel}), \\ \kappa &= \frac{1}{2}(\Gamma_{\perp} - \Gamma_{\parallel}). \end{aligned} \tag{3}$$

The same reference gives the parameters Γ_{\perp} and Γ_{\parallel} depending on the distance between the PN and the quantum system. Thus, a dynamic control of the optical properties of the medium can be achieved via varying the parameter d , which in turn changes the magnitudes of γ and κ . The susceptibility of the medium can be derived by the equations:

$$\chi_p = \frac{N\mu_{13}^2}{\epsilon_0 \hbar} \chi, \tag{4}$$

$$\chi = \frac{a_3 a_0^*}{\Omega_p} = - \frac{(A_4 + i\kappa \frac{(\Omega_c + \Omega_v)}{\Omega_p} e^{i\phi})(A_3^* A_4^* + \kappa^2)}{B}. \tag{5}$$

Here $B = (A_3 A_4 + \kappa^2)(A_3^* A_4^* + \kappa^2) + \Omega_p^2(A_4 A_4^* + \kappa^2) + (\Omega_c + \Omega_v)^2(A_3 A_3^* + \kappa^2) + 2(\Omega_c + \Omega_v)\Omega_p(\gamma + \gamma')$, N represents the atomic density, ϵ_0 is the dielectric constant in vacuum, while $A_3 = \delta_2 + i(\gamma + \gamma')$ and $A_4 = \delta_1 + i(\gamma + \gamma')$.

Following Eq. 1 we can write:

$$\Omega_c + \Omega_v = \Omega[\sin(\pi x/\Lambda_x) + \sin(\pi y/\Lambda_y) + e^{-r^2/w^2} (r/w)^{|l|} e^{i\phi}]. \tag{6}$$

We can simplify things by setting $\Omega_c + \Omega_v = \Omega = \alpha\Omega_p$, which is valid when both the probe and the coupling fields are weak. The self-Kerr nonlinearity can be obtained after the following expansion of the probe susceptibility χ_p :

$$\chi_p = \frac{N\mu_{13}^2}{\epsilon_0 \hbar} [\chi^{(1)} + \Omega_p^2 \chi^{(3)}]. \tag{7}$$

In the above, $\chi^{(1)}$ and $\chi^{(3)}$ are the first-order linear and the third-order self-Kerr nonlinear susceptibilities:

$$\begin{aligned}\chi^{(1)} &= \chi|_{(\Omega_p=0)} = -\frac{A_4 + i\alpha\kappa}{A_3 A_4 + \kappa^2}, \\ \chi^{(3)} &= \frac{d^2 \chi}{d\Omega_p^2}|_{(\Omega_p=0)} = \frac{[|A_4|^2 + \alpha^2 |A_3|^2 + \kappa^2(1 + \alpha^2) + 2\alpha(\gamma + \gamma')][A_4 + i\alpha\kappa]}{|(A_3 A_4 + \kappa^2)|^3}.\end{aligned}\quad (8)$$

In Eq. 8 we perform the transformation $\alpha \rightarrow \beta[\sin(\pi x/\Lambda_x) + \sin(\pi y/\Lambda_y) + e^{-r^2/w^2}(r/w)^{|l|}e^{il\phi}]$ with $\alpha = \frac{|\Omega|}{|\Omega_p|}$.

The theoretical model outlined in this section will serve as a basis for our studies of the azimuthal modulation of the optical properties of the quantum system under investigation.

Due to spatial position dependence of the coupling light, the quantum system acts as a two-dimensional grating and therefore the probe light diffracts into high-order directions. The diffraction pattern of the probe light can be obtained by using similar methods to those of Ref. [18], which we have followed also in our recent EIG studies [33, 47]. By using the polarization of the medium $\mathbf{P}_p = \epsilon_0 \chi \mathbf{E}_p$, we get the transmission function of the quantum system with interaction length L in the z direction:

$$T(x, y) = e^{-Im(\chi)L} e^{iRe(\chi)L}. \quad (9)$$

Further, by considering $\chi^{(1)}$ and $\chi^{(3)}$ in Eq. 8, we arrive at:

$$T(x, y) = e^{-Im(\chi^{(1)} + \Omega_p^2 \chi^{(3)})L} e^{iRe(\chi^{(1)} + \Omega_p^2 \chi^{(3)})L}, \quad (10)$$

where the first and the second terms represent the amplitude and the phase grating, respectively. The Fourier transformation of the transmission function $T(x, y)$ gives the probe field Fraunhofer diffraction:

$$K_p(\theta_x, \theta_y) = |H(\theta_x, \theta_y)|^2 \frac{\sin^2(M\pi R_x \sin \theta_x) \sin^2(N\pi R_y \sin \theta_y)}{M^2 N^2 \sin^2(\pi R_x \sin \theta_x) \sin^2(\pi R_y \sin \theta_y)}. \quad (11)$$

In the above we have used the integral expressions:

$$\begin{aligned}H(\theta_x, \theta_y) &= \int_0^1 \exp(-i2\pi x R_x \sin \theta_x) dx \int_0^1 T(x, y) \\ &\times \int_0^1 \exp(-i2\pi y R_y \sin \theta_y) dy.\end{aligned}\quad (12)$$

The angles of diffraction relative to the z direction are given by θ_x and θ_y , while $M(N)$ show the number of space periods of the grating along the $x(y)$ axis. In this case, we have $M = R_x \sin \theta_x$ and $N = R_y \sin \theta_y$, respectively.

The PN used in our work consists of spherical dielectric nanoparticles arranged in two-dimensions and coated with a metal. The radius of each sphere is $S = c/\omega_p$, the core radius is $S_c = 0.7c/\omega_p$ and the lattice constant of the square lattice is $a = 2c/\omega_p$. The relative permittivity of the shell is a Drude-form function written as:

$$\epsilon(\omega) = 1 - \frac{\omega_p^2}{\omega(\omega + i/\tau)}, \quad (13)$$

where ω_p represents the bulk plasma frequency and τ describes the relaxation time of the electrons in the metal $\tau^{-1} = 0.05\omega_p$. We also take the relative permittivity of the dielectric (SiO_2) as $\epsilon = 2.1$.

3 Results and discussion

In this section we study the vortex induced phase grating via controlling the vortex field azimuthal angle for various distances d between the PN and the quantum system. We assume two different conditions for the distances. In the first one, we consider the close distances between the PN and the quantum system (when $d = 0.1\omega_p/c = 2.2\text{nm}$) and in the second we consider the far distances (when $d = \omega_p/c = 22\text{nm}$).

For the purposes of our studies we choose the condition $\omega_{43} = 0$, e.g., a small energy gap between states $|3\rangle$ and $|4\rangle$. Table 1 shows the dependence of the spontaneous decay rates Γ_{\perp} and Γ_{\parallel} on the parameter d at transition frequency $\tilde{\omega} = 0.632\omega_p$ as based on Ref. [14], where the spontaneous decay rate in vacuum Γ_0 is used as a unit.

3.1 Amplitude and phase modulations

Figure 2 shows the amplitude modulation of the transmission function vs x and y for various distances between the PN and the quantum system when the OAM number of the vortex light equals to zero, i.e., $l = 0$. We realize that when the PN is close to the quantum system ($d = 2.2\text{nm}$), the amplitude modulation is weak, while when the system is far ($d = 22\text{nm}$) the amplitude

Table 1 Dependence of the spontaneous decay rates Γ_{\perp} and Γ_{\parallel} on the distance d between the PN and the quantum system

| Distance d (in nm) | Γ_{\perp} (in units Γ_0) | Γ_{\parallel} (in units Γ_0) |
|----------------------|---|---|
| 2.2 | 35.668 | 0.086 |
| 6.6 | 8.080 | 0.015 |
| 19.8 | 0.277 | 0.0008965 |
| 22 | 0.183 | 0.0044 |

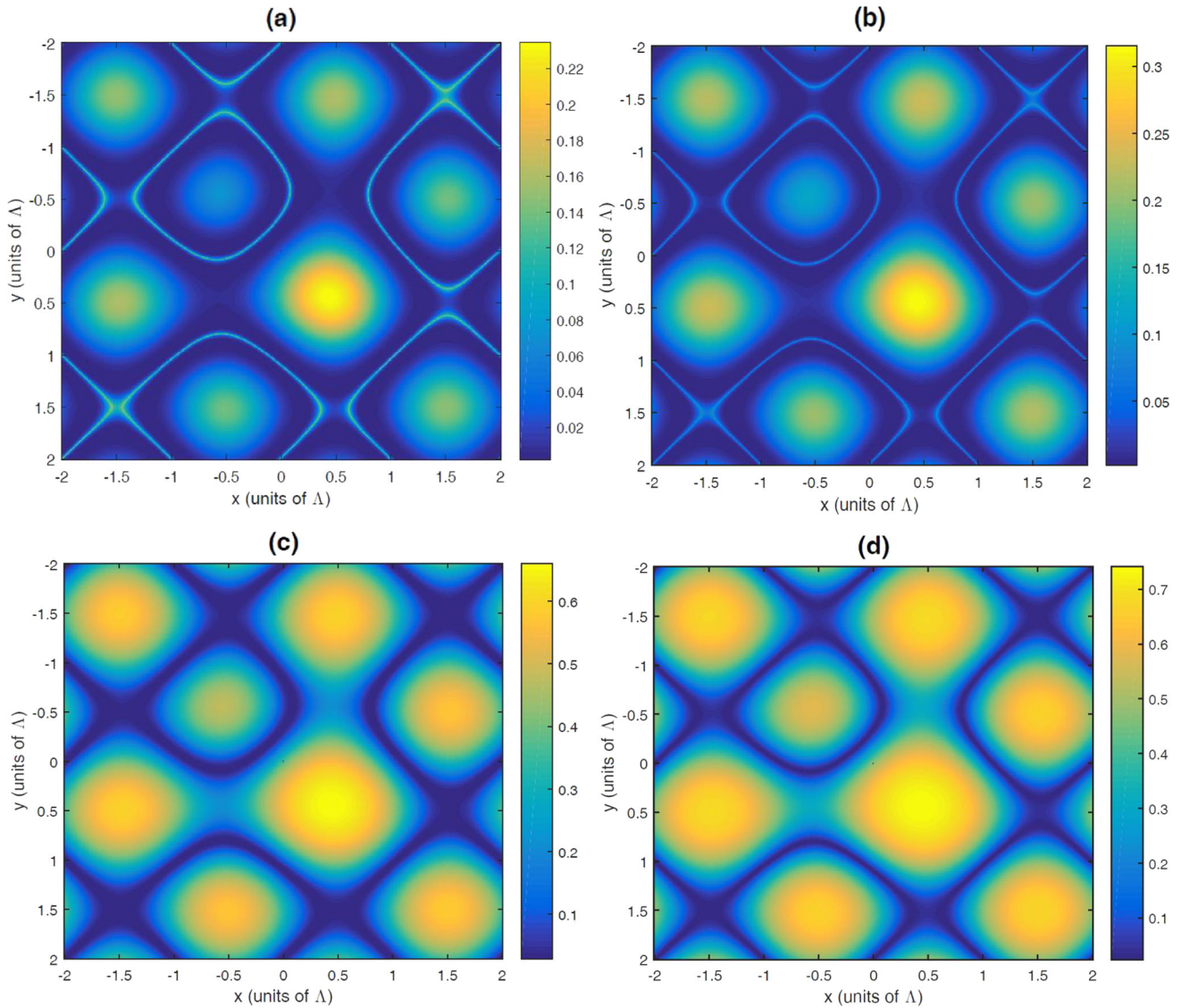


Fig. 2 Amplitude modulation vs x and y for: **a** $d = 2.2$ nm; **b** $d = 6.6$ nm; **c** $d = 19.8$ nm, and **d** $d = 22$ nm. The selected parameters are $\gamma' = 0.3$, $\delta = 0$, $\omega_{43} = 0$, $\alpha = 15$, $\omega = 1$, and $l = 0$

modulation becomes stronger. In this case, the transmission function phase modulation is zero for different distances d . A significant part of the probe energy gathers in the diffraction patterns of the zero order, while by altering d the intensity of the zero order increases.

Figure 3 represents the amplitude modulation vs x and y for a value $l = 1$ of the OAM number, while the distance between the PN and the quantum system is varied again. Here we observe that the intensity of the amplitude modulation increases with d , however this intensity is weaker than in the previous case when the winding number assumed the value $l = 0$. Further, we turn our attention to the behavior of the phase modulations of the transmission function. Figure 4 displays the phase modulation of the transmission function vs x and y for the same parametric conditions of the system as in Fig. 3. As can be seen, the phase modulation reveals certain changes depending on the distance between the PN and the quantum system. The phase modulation has a maximum value for $d = 22$ nm (Fig. 4d), while it exhibits a minimum for the small distance $d = 2.2$ nm. The latter demonstrates that part

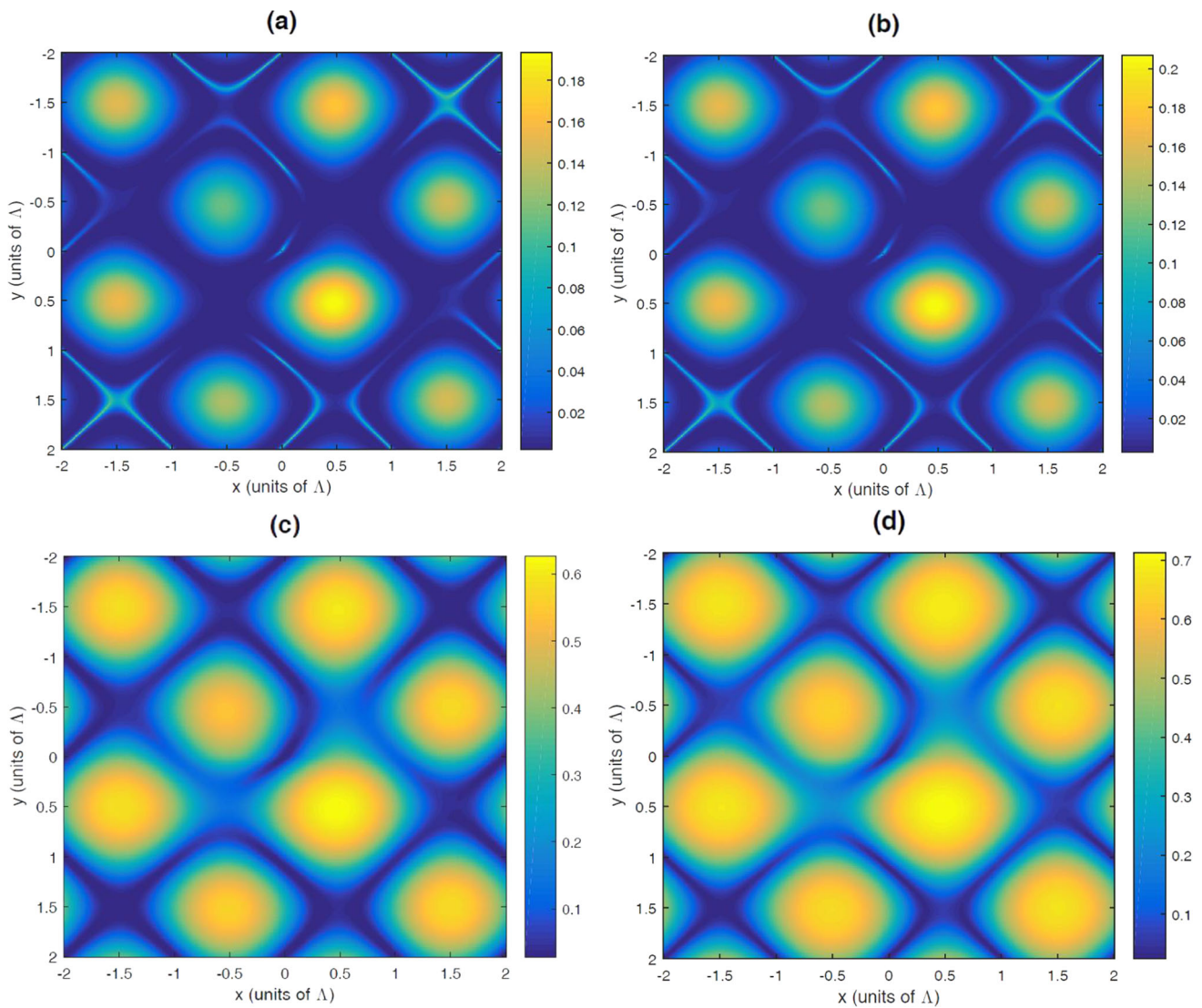


Fig. 3 Amplitude modulation vs x and y for: **a** $d = 2.2$ nm; **b** $d = 6.6$ nm; **c** $d = 19.8$ nm, and **d** $d = 22$ nm. The selected parameters are $\gamma' = 0.3$, $\delta = 0$, $\omega_{43} = 0$, $\alpha = 15$, $\omega = 1$, and $l = 1$

of the energy of the probe field is transferred to the higher orders of the grating from the zero order. Physically, for $l = 0$ we have a Gaussian light beam which leads to modulations only in the absorption spectrum of the probe light by changing the parameter d . However, for the case $l = 1$ the Laguerre–Gaussian (LG) light beam can impact both the probe field absorption and dispersion when the PN is situated at different distances from the quantum system. In other words, for a Gaussian light beam the dispersion of the quantum system becomes zero for any d , while the LG light beam causes nonzero dispersion for different distances. Thus, for $l = 0$ most of the probe energy should stay in the zero order for any value of d , while when using light with OAM the probe energy may be transferred to the higher orders of diffraction.

3.2 Fraunhofer diffraction

As a next step, in this subsection we focus on investigating the behavior of the Fraunhofer diffraction under different parameters of the system. Figure 5 shows the Fraunhofer diffraction pattern for OAM number $l = 0$ when the PN is located at different values of d from the quantum system. We find that for any d all of the probe energy gathers in the zero order and the intensities of the high orders have completely vanished. Only the intensity of the zero order increases when the parameter d is altered. We can conclude that in this case only an amplitude grating is observed and only the zero order intensity is enhanced due to presence of the PN.

Further, in Fig. 6 we study the role of altering the OAM number of the structured field on the Fraunhofer diffraction patterns when the quantum system is at $d = 2.2$ nm from the PN. We observe that for case (a), part of the energy of the probe beam is transferred from the zero order to higher orders, while some energy still stays in the zero order. The latter indicates that we have created an asymmetric

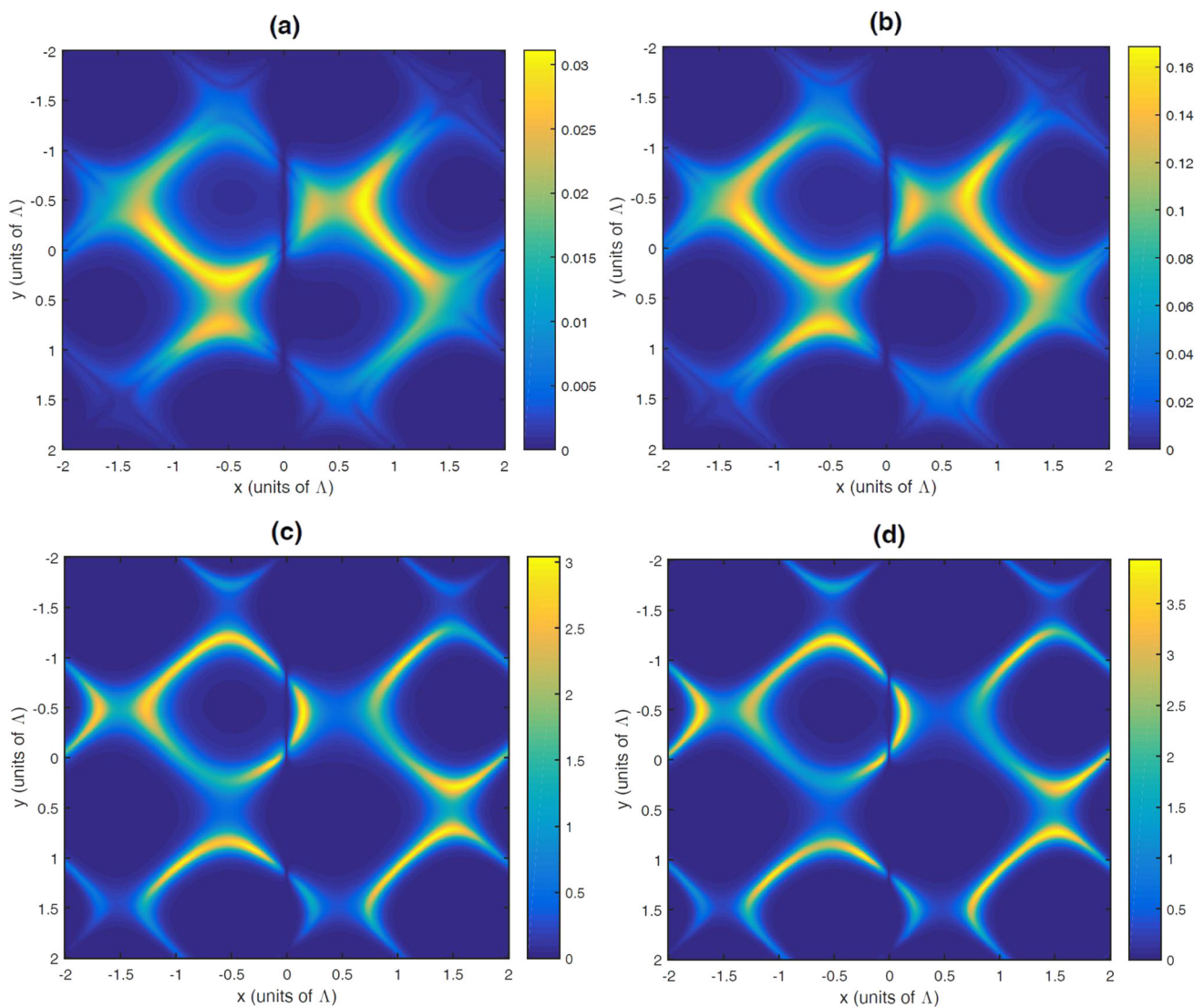


Fig. 4 Phase modulation vs x and y for: **a** $d = 2.2$ nm; **b** $d = 6.6$ nm; **c** $d = 19.8$ nm, and **d** $d = 22$ nm. The selected parameters are $\gamma' = 0.3$, $\delta = 0$, $\omega_{43} = 0$, $\alpha = 15$, $\omega = 1$, and $l = 1$

grating, where most of the energy of the probe converges in the region $-0.5 \leq \sin \theta_x \leq 0$; $0 \leq \sin \theta_y \leq 0.5$. For $l = -1$ we have the same behavior, however this time the main part of the probe energy is gathered in the region $0 \leq \sin \theta_x \leq 0.5$; $-0.5 \leq \sin \theta_y \leq 0$. Similar results are obtained for the rest of the winding number values $l = \pm 2, \pm 3, \pm 4$.

Finally, Fig. 7 displays the pattern of the Fraunhofer diffraction for a distance $d = 19.8$ nm while varying the OAM number of the LG field. In this case more of the probe field energy converges to the zero order, while just a slight portion transfers to the first order by changing l . As a result, again we have created an asymmetric grating for the different values of l .

Here we find that for both positive and negative values of the OAM number, the diffracted field could be switched from one region to another. The regions for positive value of the OAM number are in reverse with the regions for a negative value of the OAM number. In another words, by altering the OAM number, the distribution of the energy of the probe may be created in different regions with different intensities at positive or negative angles. The latter gives us the opportunity to create an asymmetric phase grating by controlling the winding number of the optical vortex light when the quantum system is located near the PN.

Considering future experimental implementations of the proposed scheme, here we suggest some realistic atomic systems with level structures exhibiting the properties required for observing the predicted effects. As the transitions from $|3\rangle$ to $|2\rangle$ (or $|1\rangle$) and $|4\rangle$ to $|2\rangle$ (or $|1\rangle$) have orthogonal dipole matrix elements, the quantum system can be realized in several atomic systems, having, for example, two $J = 0$ states for the lower states, $|1\rangle$ and $|2\rangle$, and $M = \pm 1$ sublevels of a $J = 1$ state for excited states $|3\rangle$ and $|4\rangle$. In addition, the quantum system may be realized in hyperfine sublevels of D -lines in alkali-metal atoms such as ^{85}Rb and ^{87}Rb [48, 49] or in dual CdSe/ZnS/CdSe quantum dots [9].

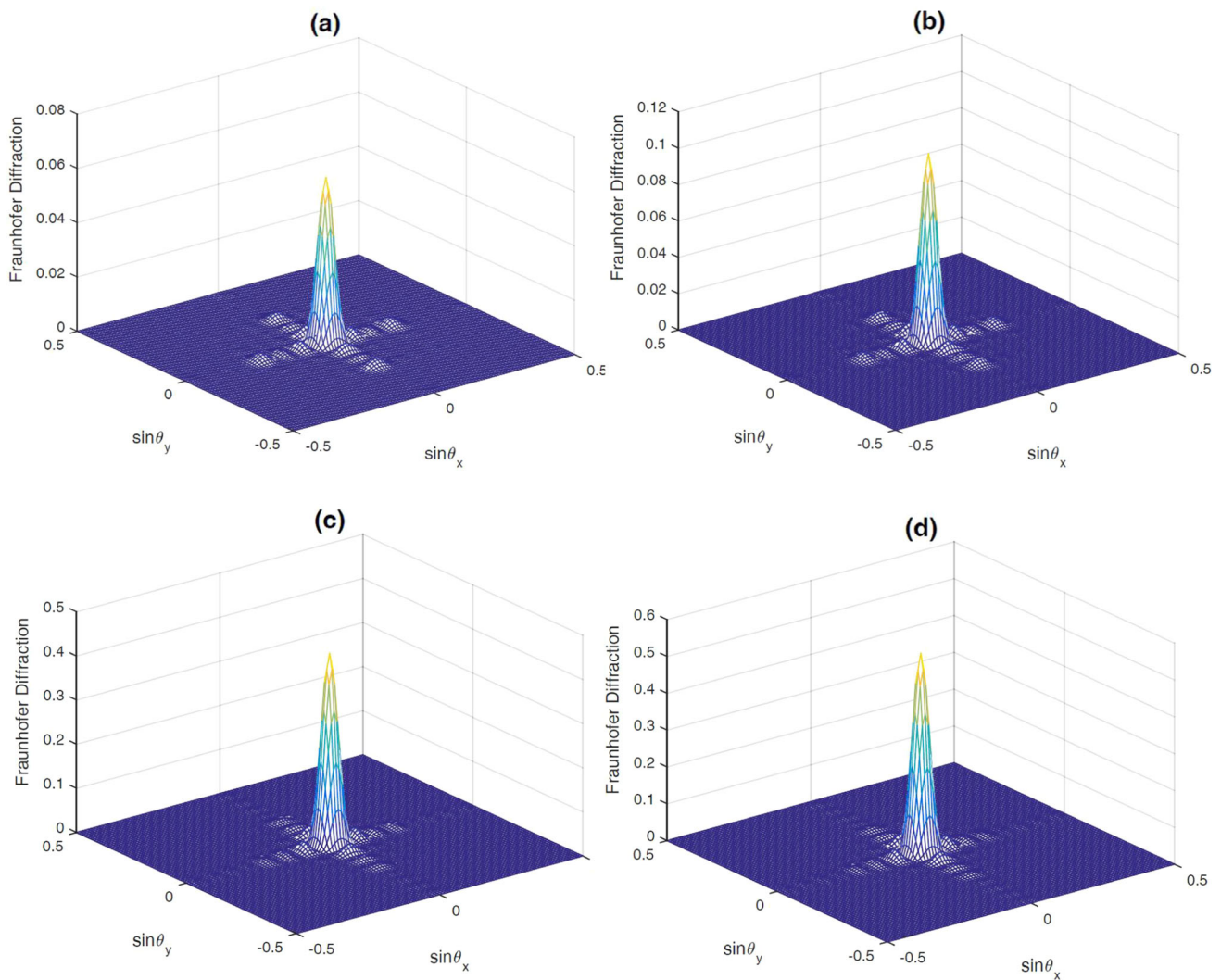


Fig. 5 Fraunhofer diffraction pattern versus $\sin \Theta_x$ and $\sin \Theta_y$ for: **a** $d = 2.2$ nm; **b** $d = 6.6$ nm; **c** $d = 19.8$ nm, and **d** $d = 22$ nm. The selected parameters are $\gamma' = 0.3$, $\delta = 0$, $\omega_{43} = 0$, $\alpha = 15$, $\omega = 1$, and $l = 0$

4 Conclusion

In summary, we have investigated the behavior of an Electromagnetically Induced Grating in a four-level quantum system located close to a plasmonic nanostructure. The system interacts with a weak probe laser field and two position-dependent standing waves and vortex lights, as a result of which a two-dimensional Electromagnetically Induced Grating is created. Our theoretical studies show that in the presence of the plasmonic nanostructure the medium is influenced by the OAM of the vortex light since it becomes phase dependent. The presented numerical simulations reveal that by varying the distance between the plasmonic nanostructure and the quantum system, the amplitude and phase modulations of the transmission function can be modified when we also alter the winding number of the vortex light. Simultaneously, we prove that when the quantum system is placed close to the plasmonic nanostructure, by adjusting the OAM of the vortex light we can transfer most of the energy of the probe to the high order, while at larger distances most of this energy is converged in the zero order. Thus, our work demonstrates a simple scheme for double control over the diffraction efficiency of the two-dimensional grating by utilizing both the winding number of the vortex field and the distance between the plasmonic nanostructure and the quantum system as control knobs. Combining the strong modifications of coherent optical phenomena occurring near plasmonic nanostructures with the additional degrees of freedom yielded by optical vortex fields, the proposed scheme is advantageous by providing easily achievable manipulation of the grating performance, while it can be realized in typical quantum optics experimental settings. For example, the accurate positioning of the quantum system and the plasmonic nanostructure can be easily controlled by adding a buffer layer/ film between the quantum system and the nanostructure, i.e., by placing the quantum system on top of this layer which is adjacent to the plasmonic nanostructure. This layer can be made of a low-index ($n \approx 1$) polymer [50], so that it does not affect the optical response of the setup of the quantum system/ plasmonic

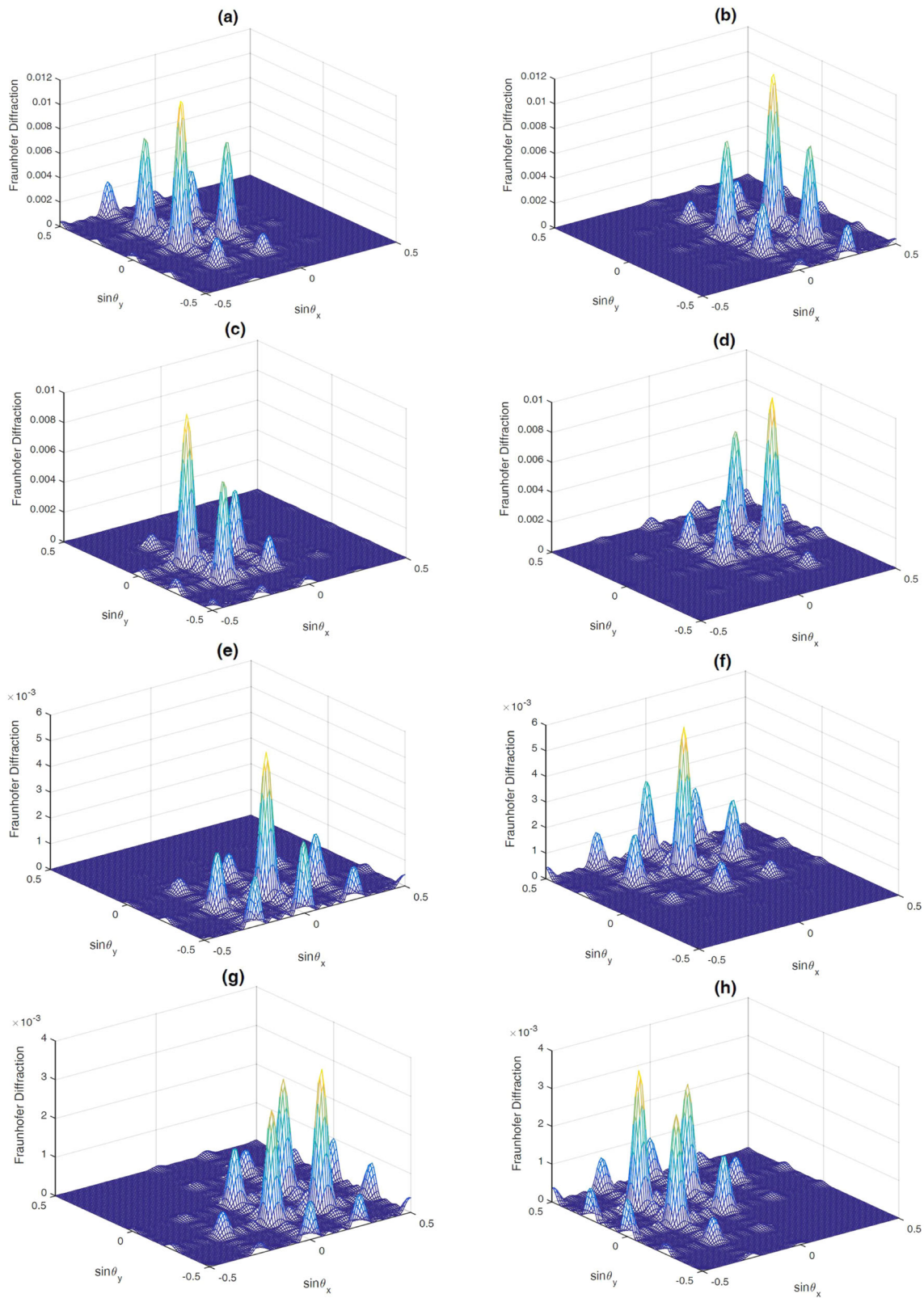


Fig. 6 Fraunhofer diffraction pattern versus $\sin \Theta_x$ and $\sin \Theta_y$ for $d = 2.2$ nm: **a** $l = 1$; **b** $l = -1$; **c** $l = 2$; **d** $l = -2$; **e** $l = 3$; **f** $l = -3$; **g** $l = 4$; **h** $l = -4$. The selected parameters are $\gamma' = 0.3$, $\delta = 0$, $\omega_{43} = 0$, $\alpha = 15$, $M = N = 4$, $L = 15$, and $\omega = 1$

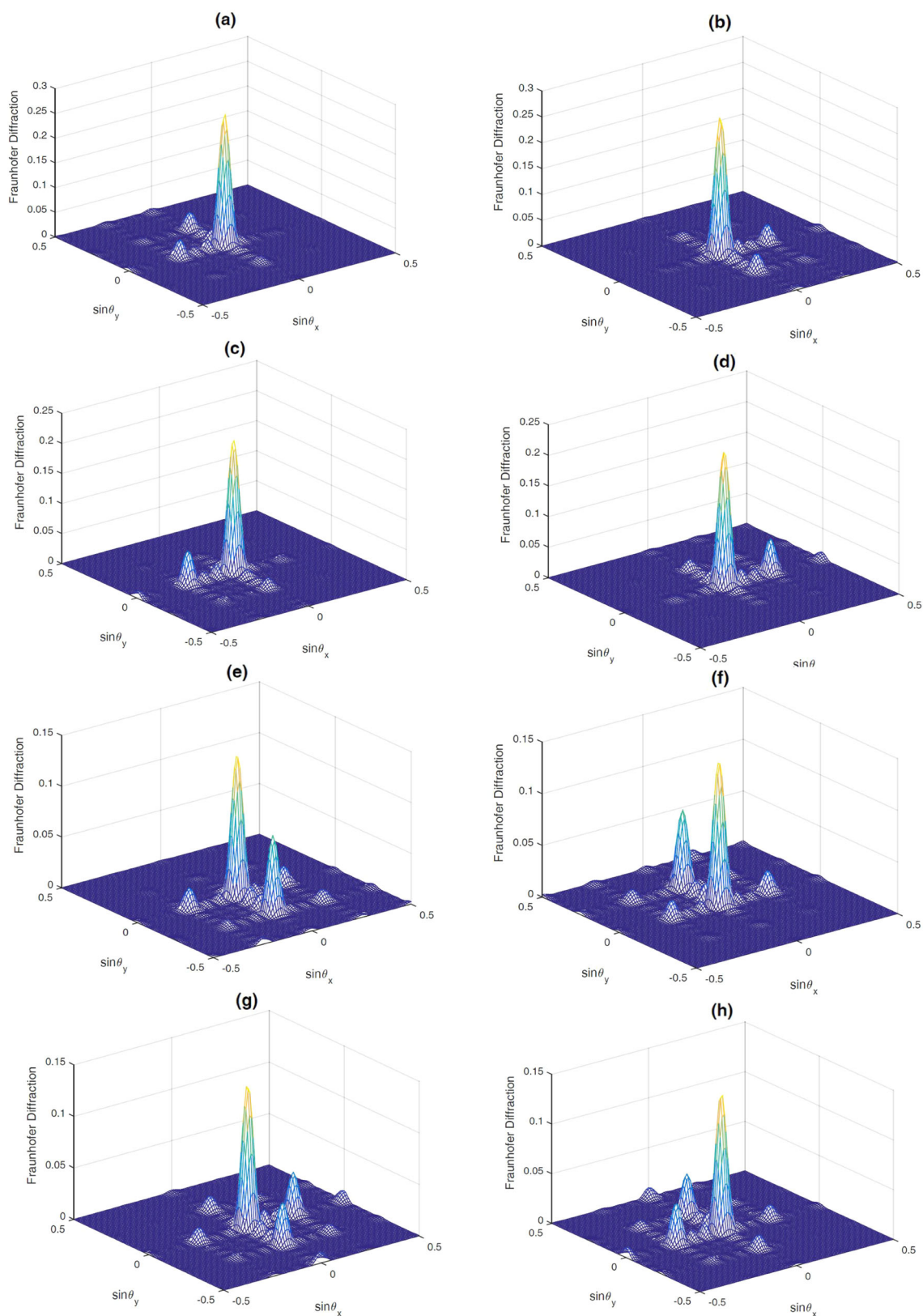


Fig. 7 Fraunhofer diffraction pattern versus $\sin\Theta_x$ and $\sin\Theta_y$ for $d = 19.8$ nm: **a** $l = 1$; **b** $l = -1$; **c** $l = 2$; **d** $l = -2$; **e** $l = 3$; **f** $l = -3$; **g** $l = 4$; **h** $l = -4$. The selected parameters are $\gamma' = 0.3$, $\delta = 0$, $\omega_{43} = 0$, $\alpha = 15$, $M = N = 4$, $L = 15$, and $\omega = 1$

nanostructure. In addition, such an atomic phase grating could be crucial for future applications in all-optical quantum switching at the few photons level, providing paramount low losses.

Author contributions EP and HRH generated the idea and designed the theoretical methods. SHA performed the numerical investigations. The results were interpreted by VY and EP. TK prepared the manuscript for publication. All authors contributed to editing the manuscript.

Funding This work was supported by a STSM Grant from COST Action CA16221 for T. Kirova and H. R. Hamed. T. Kirova received support from the Grant No. LV-LT-TW/2022/4 “Coherent Optical Control of Atomic Systems” by the Ministry of Education and Science of the Republic of Latvia. H. R. Hamed acknowledges support from the Grant No. S-LLT-22-2 “Coherent Optical Control of Atomic Systems” by the Lithuanian Council of Research.

Data Availability Statement This manuscript has associated data in a data repository. [Authors’ comment: All data included in this manuscript are available upon request by contacting the corresponding author.]

Declarations

Conflict of interest The authors declare that they have no conflict of interest.

References

- H.A. Atwater, A. Polman, Plasmonics for improved photovoltaic devices. *Nat. Mater.* **9**, 205–213 (2010)
- M.W. Knight, H. Sobhani, P. Nordlander, N.J. Halas, Photodetection with active optical antennas. *Science* **332**(6030), 702–704 (2011)
- N. Liu, M.L. Tang, M. Hentschel, H. Giessen, A.P. Alivisatos, Nanoantenna-enhanced gas sensing in a single tailored nanofocus. *Nat. Mater.* **10**, 631–636 (2011)
- D. Boyer, P. Tamarat, A. Maali, B. Lounis, M. Orrit, Photothermal imaging of nanometer-sized metal particles among scatterers. *Science* **297**(5584), 1160–1163 (2002)
- K.A. Willets, R.P. Van Duyne, Localized surface plasmon resonance spectroscopy and sensing. *Ann. Rev. Phys. Chem.* **58**, 267–297 (2007)
- E.R. Corson, E.B. Creel, R. Kostecki, B.D. McCloskey, J.J. Urban, Important considerations in plasmon-enhanced electrochemical conversion at voltage-biased electrodes. *iScience*, **23**, 100911-1–100911-10 (2020)
- W. Ou, B. Zhou, J. Shen, Ch. Zhao, Y.Y. Li, J. Lu, Plasmonic metal nanostructures: concepts, challenges and opportunities in photo-mediated chemical transformations. *iScience* **24**, 101982-1–101982-17 (2021)
- S. Evangelou, V. Yannopapas, E. Paspalakis, Transparency and slow light in a four-level quantum system near a plasmonic nanostructure. *Phys. Rev. A* **86**, 053811-1–053811-9 (2012)
- L. Wang, Y. Gu, H. Chen, J.-Y. Zhang, Y. Cui, B.D. Gerardot, Q. Gong, Polarized linewidth-controllable double-trapping electromagnetically induced transparency spectra in a resonant plasmon nanocavity. *Sci. Rep.* **3**, 2879-1–2879-7 (2013)
- J.D. Cox, M.R. Singh, C. von Bilderling, A.V. Bragas, A nonlinear switching mechanism in quantum dot and metallic nanoparticle hybrid systems. *Adv. Opt. Mater.* **1**(6), 460–467 (2013)
- M.R. Singh, Enhancement of the second-harmonic generation in a quantum dot-metallic nanoparticle hybrid system. *Nanotechnology* **24**(12), 125701 (2013)
- M.A. Antón, F. Carreño, S. Melle, O.G. Calderón, E. Cabrera-Granado, M.R. Singh, Optical pumping of a single hole spin in a p-doped quantum dot coupled to a metallic nanoparticle. *Phys. Rev. B* **87**, 195303-1–195303-13 (2013)
- E. Paspalakis, S. Evangelou, A.F. Terzis, Control of excitonic population inversion in a coupled semiconductor quantum dot-metal nanoparticle system. *Phys. Rev. B* **87**, 235302-1–235302-6 (2013)
- E. Paspalakis, S. Evangelou, V. Yannopapas, A.F. Terzis, Phase-dependent optical effects in a four-level quantum system near a plasmonic nanostructure. *Phys. Rev. A* **88**, 053832-1–053832-8 (2013)
- D. Bortman-Arbiv, A.D. Wilson-Gordon, H. Friedmann, Phase control of group velocity: from subluminal to superluminal light propagation. *Phys. Rev. A* **63**, 043818-1–043818-7 (2001)
- J.-H. Wu, J.-Y. Ga, Phase control of light amplification without inversion in a Λ system with spontaneously generated coherence. *Phys. Rev. A* **65**, 063807-1–063807-5 (2002)
- W.-H. Xu, J.-H. Wu, J.-Y. Gao, Effects of spontaneously generated coherence on transient process in a Λ system. *Phys. Rev. A* **66**, 063812-1–063812-6 (2002)
- H.-Y. Ling, Y.-Q. Li, M. Xiao, Electromagnetically induced grating: homogeneously broadened medium. *Phys. Rev. A* **57**(2), 1338–1344 (1998)
- M. Mitsunaga, N. Imoto, Observation of an electromagnetically induced grating in cold sodium atoms. *Phys. Rev. A* **59**(6), 4773–4776 (1999)
- G.C. Cardoso, J.W.R. Tabosa, Electromagnetically induced gratings in a degenerate open two-level system. *Phys. Rev. A* **65**, 033803-1–033803-7 (2002)
- S.E. Harris, J.E. Field, A. Imamoglu, Nonlinear optical processes using electromagnetically induced transparency. *Phys. Rev. Lett.* **64**(10), 1107–1110 (1990)
- M. Fleischhauer, A. Imamoglu, J.P. Marangos, Electromagnetically induced transparency. *Rev. Mod. Phys.* **77**, 633–637 (2005)
- D. Moretti, D. Felinto, J. Tabosa, A. Lezama, Dynamics of a stored Zeeman coherence grating in an external magnetic field. *J. Phys. B At., Mol. Opt. Phys.* **43**, 115502-1–115502-7 (2010)
- A.W. Brown, M. Xiao, All-optical switching and routing based on an electromagnetically induced absorption grating. *Opt. Lett.* **30**(7), 699–701 (2005)
- L. Zhao, W. Duan, S.F. Yelin, All-optical beam control with high speed using image-induced blazed gratings in coherent media. *Phys. Rev. A* **82**, 013809-1–013809-8 (2010)
- P.W. Zhai, X.M. Su, J.Y. Gao, Optical bistability in electromagnetically induced grating. *Phys. Lett. A* **289**, 27–33 (2001)
- F. Wen, W. Wang, I. Ahmed, H. Wang, Y. Zhang, Y. Zhang, A.R. Mahesar, M. Xiao, Two-dimensional Talbot self-imaging via electromagnetically induced lattice. *Sci. Rep.* **7**, 41790-1–41790-9 (2017)
- Y. Zhang, Ch. Yuan, Y. Zhang, H. Zheng, H. Chen, Ch. Li, Zh. Wang, M. Xiao, Surface solitons of four-wave mixing in an electromagnetically induced lattice. *Laser Phys. Lett.* **10**, 055406-1–055406-5 (2013)

29. S. Franke-Arnold, J. Leach, M.J. Padgett, V.E. Lembessis, D. Ellinas, A.J. Wright, J.M. Girkin, P. Öhberg, A.S. Arnold, Optical ferris wheel for ultracold atoms. *Opt. Express* **15**(14), 8619–8625 (2007)
30. X. He, P. Xu, J. Wang, M. Zhan, Rotating single atoms in a ring lattice generated by a spatial light modulator. *Opt. Express* **17**(23), 21007–21014 (2009)
31. L. Wang, F. Zhou, P. Hu, Y. Niu, Sh. Gong, Two-dimensional electromagnetically induced cross-grating in a four-level tripod-type atomic system. *J. Phys. B At. Mol. Opt. Phys.* **47**(22), 013838-1–013838-7 (2014)
32. T. Naseri, R. Sadighi-Bonabi, Electromagnetically induced phase grating via population trapping condition in a microwave-driven four-level atomic system. *J. Opt. Soc. Am. B* **31**, 2879–2884 (2014)
33. S.H. Asadpour, H.R. Hamed, T. Kirova, E. Paspalakis, Two-dimensional electromagnetically induced phase grating via composite vortex light. *Phys. Rev. A* **105**, 043709-1–043709-11 (2022)
34. D.L. Andrews, M. Babiker, *The Angular Momentum of Light* (Cambridge University Press, Cambridge, 2012)
35. G. Molina-Terriza, J.P. Torres, L. Torner, Twisted photons. *Nat. Phys.* **3**, 305–310 (2007)
36. J. Wang, Advances in communications using optical vortices. *Photon. Res.* **5**, B14–B28 (2016)
37. H.R. Hamed, J. Ruseckas, E. Paspalakis, G. Juzeliūnas, Transfer of optical vortices in coherently prepared media. *Phys. Rev. A* **99**(3), 053822-1–053822-5 (2019)
38. H.R. Hamed, E. Paspalakis, G. Zlabys, G. Juzeliūnas, J. Ruseckas, Complete energy conversion between light beams carrying orbital angular momentum using coherent population trapping for a coherently driven double-Lambda atom-light-coupling scheme. *Phys. Rev. A* **100**, 023811-1–023811-8 (2019)
39. Z. Dutton, J. Ruostekoski, Transfer and storage of vortex States in light and matter waves. *Phys. Rev. Lett.* **93**, 193602-1–193602-4 (2004)
40. J. Ruseckas, G. Juzeliūnas, P. Öhberg, Polarization rotation of slow light with orbital angular momentum in ultracold atomic gases. *Phys. Rev. A* **76**, 053822-1–053822-5 (2007)
41. S.H. Asadpour, A. Panahpour, M. Jafari, Phase-dependent electromagnetically induced grating in a four-level quantum system near a plasmonic nanostructure. *Eur. Phys. J. Plus*, **133**, 411-1–411-7 (2018)
42. H.R. Hamed, V. Yannopapas, E. Paspalakis, Spatially structured optical effects in a four-Level quantum system near a plasmonic nanostructure. *Ann. Phys.* **533**, 2100117 (2021)
43. V. Yannopapas, E. Paspalakis, N.V. Vitanov, Plasmon-induced enhancement of quantum interference near metallic nanostructures. *Phys. Rev. Lett.* **103**, 063602-1–063602-4 (2009)
44. S. Evangelou, V. Yannopapas, E. Paspalakis, Modifying free-space spontaneous emission near a plasmonic nanostructure. *Phys. Rev. A* **83**, 023819-1–023819-7 (2011)
45. S. Evangelou, V. Yannopapas, E. Paspalakis, Simulating quantum interference in spontaneous decay near plasmonic nanostructures: population dynamics. *Phys. Rev. A* **83**, 055805-1–055805-4 (2011)
46. H. Yan, K.-Y. Liao, J.-F. Li, Y.-X. Du, Zh.-M. Zhang, Sh.-L. Zhu, Bichromatic electromagnetically induced transparency in hot atomic vapors. *Phys. Rev. A* **87**, 055401-1–055401-5 (2013)
47. S.H. Asadpour, T. Kirova, J. Qia, H.R. Hamed, G. Juzeliūnas, E. Paspalakis, Azimuthal modulation of electromagnetically induced grating using structured light. *Sci. Rep.* **11**, 20721-1–20721-11 (2021)
48. Y. Gu, L. Wang, P. Ren, J.-X. Zhang, T.-C. Zhang, O.J.F. Martin, Q.-H. Gong, Surface-plasmon-induced modification on the spontaneous emission spectrum via subwavelength-confined anisotropic Purcell factor. *Nano Lett.* **12**, 2488–2493 (2012)
49. M. Sukharev, S.A. Malinovskaya, Stimulated Raman adiabatic passage as a route to achieving optical control in plasmonics. *Phys. Rev. A* **86**, 043406-1–043406-7 (2012)
50. A.A. Hashim, *Polymer Thin Films* (IntechOpen, London, 2010)

Springer Nature or its licensor (e.g. a society or other partner) holds exclusive rights to this article under a publishing agreement with the author(s) or other rightsholder(s); author self-archiving of the accepted manuscript version of this article is solely governed by the terms of such publishing agreement and applicable law.